Thompson, E. B., Kies, M. W., and Alvord, E. C., Jr. (1963), *Biochem. Biophys. Res. Commun. 13*, 198.
Thorun, W., and Mehl, E. (1968), *Biochim. Biophys. Acta 160*, 132.
Tung, J. S., and Knight, C. A. (1971), *Biochem. Biophys. Res. Commun. 42*, 1117.
Ugel, A. R., Chrambach, A., and Rodbard, D. (1971), *Anal. Biochem. 43*, 410.
Waehneldt, T. V., and Mandel, P. (1970), *FEBS (Fed. Eur. Biochem. Soc.) Lett. 9*, 209.
Weber, K., and Osborne, M. (1969), *J. Biol. Chem. 244*, 4406.

Study of *Escherichia coli* Ribosomes by Intensity Fluctuation Spectroscopy of Scattered Laser Light†

Dennis E. Koppel*

ABSTRACT: The ribosomes of *Escherichia coli* have been studied by the technique of light-scattering intensity fluctuation spectroscopy. A digital photocount correlator was used to analyze the time evolution of the scattered field and thus characterize the hydrodynamic properties of the ribosomes in solution with accurate determinations of *D*, the translational diffusion coefficient. To selectively study the molecules of interest, the light-scattering technique was combined with the technique of band or zonal sedimentation in a sucrose gradient. The light-scattering experiments were carried out immediately after centrifugation directly on the different macromolecular bands in the sucrose gradient in the centrifuge tube. The values of $D^{\circ}_{20,\mathrm{w}}$ determined in this way are $(1.71 \pm 0.03) \times 10^{-7}$ cm^2/sec, $(1.90 \pm 0.03) \times 10^{-7}$ cm^2/sec, and $(2.18 \pm 0.03) \times 10^{-7}$ cm^2/sec for the 70S ribosomes and the 50S and 30S ribosome subunits, respectively. Combining these measured values of *D* with literature values of the sedimentation coefficients and partial specific volumes, values of the ribosome molecular weights were calculated. These are, in millions, 2.49 ± 0.06, 1.55 ± 0.04, and 0.87 ± 0.02, in the same order as above. Finally, the results of this work were compared to those of other techniques, and discussed in terms of the size, shape, and degree of hydration of the ribosome molecules.

In the work reported here, the ribosomes of *Escherichia coli* are studied by the technique of laser light scattering IFS[1] (see, for example, Clark *et al.*, 1970; Cummins and Swinney, 1970; Chu, 1970; Foord *et al.*, 1970; Pusey *et al.*, 1974). IFS is a recently developed technique in which the coherent radiation of a laser light source is used to probe the dynamics of systems of scatters, in this case, biological macromolecules in solution. The field from each scatterer acts as a reference signal with which we can detect the phase fluctuations in the field from each other scatterer. Molecular motions over distances of the order of a wavelength of light change the relative phases at the detector of the scattered electric field from different scattering centers, thus changing the detected light intensity. The coherence time of the scattered light, the characteristic time scale on which light intensity fluctuates, is thus directly related to the hydrodynamic properties of the scattering molecules. In this study, we used a digital photocount correlator to analyze the scattered field.

For scatterers of linear dimensions small compared to a wavelength of light, such as those studied here, the coherence time of the scattered field is inversely proportional to *D*, the macromolecular translational diffusion coefficient (Pecora, 1964). For nonspherical molecules of linear dimensions comparable to a wavelength of light, one can investigate rotational diffusion (Pecora, 1968; Cummins *et al.*, 1969; Schaefer *et al.*, 1971), and internal molecular flexing modes (Pecora, 1965; Fujime, 1970).

As a general analytical technique, however, IFS has two inherent limitations.

i. Lack of Specificity. All solute particles, desired and undesired, scatter light. The greatest damage can be done by large aggregates and dust, which, even in minute concentrations, can swamp the signal from the molecules of interest.

ii. Poor Resolution of Different Components. Light-scattering data are relatively insensitive to solution polydispersity. The best one can do in general (Koppel, 1972; Pusey *et al.*, 1974) is to calculate the first two or three moments of the distribution of molecular size (actually the distribution of *D*); but additional information is needed for a detailed characterization.

In an attempt to overcome the above limitations, the work reported here combines IFS with the technique of band or zonal sedimentation in the ultracentrifuge. For other techniques as well as for light-scattering measurements, band sedimentation on a sucrose gradient has frequently been used as one of the final sample preparative procedures. Traditionally, fractions are collected, dialyzed against buffer to remove the sucrose, and analyzed separately. The experimental work reported here takes the next logical step: The light-scattering analysis is carried out immediately after centrifugation directly on the different macromolecular bands in the sucrose gradient in the centrifuge tube. One can thus selectively study the molecules of interest, separated from a host of other potential scatterers, with an ease and reliability not previously possible.

---

† From the Department of Physics, Columbia University, New York, N. Y. 10027, and the IBM Thomas J. Watson Research Center, Yorktown Heights, New York 10598.

* To whom to address correspondence at the School of Applied and Engineering Physics, Cornell University, Ithaca, N. Y. 14850.

[1] Abbreviation used is: IFS, intensity fluctuation spectroscopy.

The ribosomes of *E. coli* are an ideal subject for this study. They are sufficiently complex to provide a good test of the technique's capabilities. They have been characterized by other techniques (see for example, Kurland, 1972; Spirin, 1969; Spirin and Gavrilova, 1969) so that a context exists within which the results of this study can be evaluated. However the gross morphological characteristics of the ribosomes (the size, shape, and degree of hydration) have yet to be firmly established (Hill *et al.*, 1969a).

Experimental Section

Sample Preparation. The ribosomes used in this study were the generous gift of Dr. Charles R. Cantor and Ms. Helen Oen, of the Department of Chemistry, Columbia University. 70S ribosomes were prepared from midlogarithmic phase *E. coli* Q13 by the method of Traub *et al.* (1971). This procedure does not include washings in high salt (*e.g.*, 1 M NH_4Cl) which will produce significant changes in the ribosome properties (Hill *et al.*, 1970). The following buffers were used: I, 0.01 M Tris-HCl (pH 7.4)–0.05 M NH_4Cl–1.0×10^{-2} M $MgCl_2$–6.0×10^{-3} M 2-mercaptoethanol; II, same as I, except 2.5×10^{-4} M $MgCl_2$. Concentrates ($\sim$50 mg/ml) of 70S particles in buffer I were stored frozen, until needed, at liquid nitrogen temperature. 30S and 50S ribosomal subunits were prepared from 70S ribosomes by dialysis against buffer II for 24 hr at 5°. It should be noted that the 30S subunit may not be active at Mg concentrations below 2 mM (Zamir *et al.*, 1971). This suggests a difference between the conformations of the subunits at low and high Mg concentrations (Ghysen *et al.*, 1970).

Typically, 2-ml volumes of solution were layered on linear 10–30%, 37-ml sucrose gradients in standard 1 in. diameter × 3.5 in. cellulose nitrate centrifuge tubes. If material is scarce, much smaller volumes of sample can be used. In fact, one can easily use sample volumes of 0.1 ml or less, considerably less than that needed with conventional light-scattering sample preparation techniques.

All centrifuge runs were performed with a swinging-bucket SW27 rotor at a temperature of $0 \pm 0.5°$. Immediately after centrifugation, the sample tube was sealed with a precooled cap of the type usually used with a fixed-angle rotor. To minimize the disturbance of the gradient the caps were specially modified, with the inner supporting cylindrical shell removed. Using the screw threads on the top of the cap, the sample tube was rigidly attached to a translational device and suspended from above into the thermal water bath of the light-scattering photometer.

Light-Scattering Experiment. A schematic diagram of the light-scattering photometer is presented in Figure 1. The incident field is provided by a Model 52 Coherent Radiation krypton ion laser. The sample tube is housed in the center of a cylindrical water bath which provides temperature control, and, through approximate index matching, a reduction of the light reflected by the tube wall. The scattering volume is imaged onto a narrow vertical slit, and the light transmitted is detected by an ITT FW130 photomultiplier tube with an effective photocathode area smaller than a coherence area of the scattered field. This means that at any given instant, there is nearly complete spatial coherence of the scattered field across the surface of the detector. If this were not the case, the intensity fluctuations that we are interested in would be spatially averaged out in the detection process.

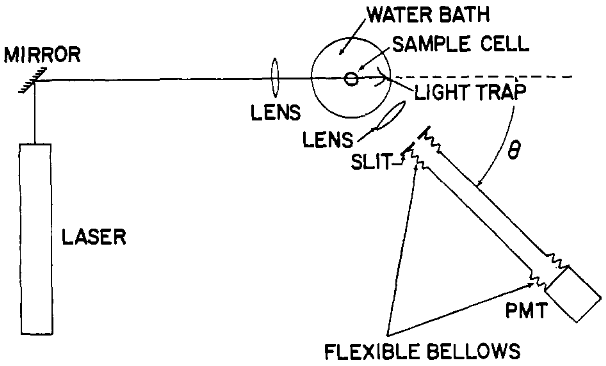

FIGURE 1: The light-scattering photometer.

The light-scattering experiment consists of two vertical translation scans of each centrifuge tube through the incident laser beam. The general approach is as follows. During the first scan, at closely spaced intervals, the average intensity of the scattered light is determined as a function of position in the tube. This gives a measure of the concentration profile of the macromolecules. With Z, the weight per cent of sucrose, known as a function of position,[2] one can determine the sedimentation coefficient corresponding to each peak in the scattering power profile with the aid of published tables (McEwen, 1967). In many applications, with well-characterized systems, these calculations are used basically as a means of identifying known components of the solution with known sedimentation coefficients, and need not be especially precise.

On the second scan through the tube, stopping at positions shown to be of interest by the first scan, photocount autocorrelation functions are measured. One thus obtains experimental values of DK^2 (see below) where D is the diffusion coefficient of the scatterers, and K is the magnitude of the scattering vector. Inasmuch as K is proportional to $\tilde{n}$, the refractive index of the scattering medium, and D is inversely proportional to η, the viscosity of the solvent, an accurate knowledge of Z at the point of measurement is all the more essential.[3]

Extrapolations to zero macromolecular concentration can be performed by lowering the concentration of the initial layer of sample solution. Combining the extrapolated diffusion and sedimentation coefficients one gets the molecular weight of each component (Svedberg and Pederson, 1940). It is then possible to convert the measured scattering power profile to a relative weight concentration profile. Absolute concentrations can be determined with the use of a light-scattering standard. After the solution has been characterized in this fashion, fractions can still be collected, if desired, for further physical or chemical analyses.

A sucrose gradient without ribosomes was used as the light scattering standard. To calibrate the standard, we utilized the relationship between the intensity of the light scattered by a solution (above that of solvent alone) and Π, the osmotic pressure (Debye, 1947)

$$\langle I \rangle = \text{const} \times c\tilde{n}_0^{\,2}(\mathrm{d}\tilde{n}/\mathrm{d}c)^2[\partial(\Pi/RT)/\partial c]^{-1} \qquad (1)$$

where c is the weight concentration of solute, $\tilde{n}_0$ is the refractive index of the solvent, R is the gas constant, and T is the

---

[2] For 37-ml sucrose gradients, with $10 \leq Z \leq 28.73$, in 1 in. diameter × 3.5 in. cellulose nitrate tubes (Beckman No. 302237), in a swinging-bucket SW27 rotor (Spinco, Palo Alto, Calif.), $Z = -10 + 2.48\ \text{cm}^{-1}\, r$, where r is the distance from the axis of rotation in the centrifuge during centrifugation (Koppel, 1973).

[3] To correct for the presence of sucrose, one must know $(\eta_{T,\mathrm{s}}/\eta_{T,\mathrm{w}})\cdot(\tilde{n}_{T,\mathrm{w}}/\tilde{n}_{T,\mathrm{s}})^2$, where s and w refer to sucrose solution and water, respectively. Viscosity data were taken from the Handbook of Biochemistry (1972). Refractive indices were from the Handbook of Chemistry and Physics (1972).

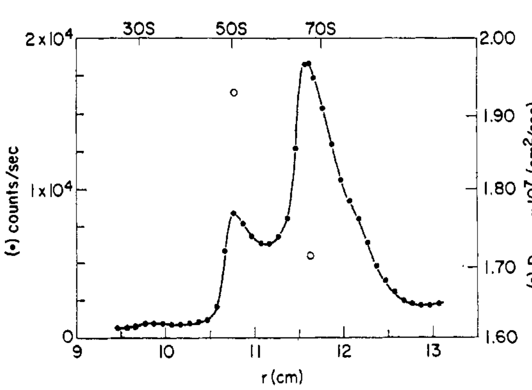

FIGURE 2: Ribosomes in buffer I, after centrifugation with $\omega = 1.903 \times 10^3\ \text{sec}^{-1}$. $\int\omega^2 dt = 1.724 \times 10^{11}\ \text{sec}^{-1}$.

absolute temperature. Sucrose solution osmotic pressure data were obtained from the International Critical Tables (1928). Differentiation with respect to concentration was performed numerically with least-squares straight line fits to all sets of four consecutive points. The value of $d\tilde{n}/dc$ for the ribosome solutions was taken from the literature (Scafati *et al.*, 1971), and corrected, in each case, for the known concentration of sucrose (Koppel, 1973).

Photocount Autocorrelation. The laser light scattered by the ribosome solutions was characterized by the technique of digital photocount autocorrelation. "Clipped" correlation (Jakeman and Pike, 1969; Foord *et al.*, 1970; Koppel, 1971) can be performed with relatively simple digital correlators, and is the method of choice of this study. One measures $\langle n_q(t)n(t + \tau)\rangle$, where the angular brackets indicate an ensemble or time average, $n(t)$ is the number of detected photons (photocounts) in a counting interval centered at time t, and $n_q(t)$, the clipped count, is defined as

$$n_q(t) = \begin{cases} 0 \text{ if } n(t) \le q \\ 1 \text{ if } n(t) > q \end{cases} \tag{2}$$

with q a nonnegative integer.

While in general the relation between the clipped function and the field statistics is exceedingly complex, for Gaussian fields,[4] it reduces to an especially simple expression (Jakeman and Pike, 1969; Koppel, 1971)

$$\langle n_q(0)n(\tau)\rangle = \langle n_q\rangle\langle n\rangle\{1 + [(1 + q)/(1 + \langle n\rangle)]Y_q|g^{(1)}(\tau)|^2\} \tag{3}$$

Here $g^{(1)}(\tau)$ is the normalized first-order electric field correlation function

$$g^{(1)}(\tau) \equiv \langle\epsilon^*(0)\epsilon(\tau)\rangle/\langle|\epsilon|^2\rangle \tag{4}$$

and Y_q (Koppel, 1971) is a constant, independent of the delay time τ, which incorporates the effects of finite sampling times and incomplete spatial coherence of the field across the photoemissive area of the detector. $|g^{(1)}(\tau)|$, in turn, is easily related to the hydrodynamic diffusion properties of the scattering molecules. For dilute solutions of macromolecules small compared to a wavelength of light and/or spherically symmetric (Pecora, 1964)

$$|g^{(1)}(\tau)| = e^{-DK^2\tau} \tag{5}$$

where K is the magnitude of the scattering vector.

In the bulk of the work reported here, experimental values for $\langle n_0(0)n(\tau)\rangle$, $\langle n\rangle$, and $\langle n_0\rangle$ were determined, and combined according to eq 3 to give estimates of $Y_0|g^{(1)}(\tau)|^2$. Taking the natural logarithm of these estimates, values of D were determined with weighted, least-squares, straight-line fits. As an occasional check of the field statistics, $\langle n_0^{(8)}(0)n(\tau)\rangle$, the prescaled clipped correlation function (Koppel and Schaefer, 1973; Jakeman *et al.*, 1972), was measured as well. Scaling before the clipping procedure effects an averaging over s consecutive clipping levels. Thus, if eq 3 applies for all clipping levels (as it must for Gaussian light), then $\langle n_0^{(8)}(0)n(\tau)\rangle$ and $\langle n_0(0)n(\tau)\rangle$ should give identical results.

Measurements can be taken at many scattering angles as a check for a variety of systematic effects: instrumental effects (*e.g.*, optical misalignment) as well as sample-specific effects (*e.g.*, an unwanted component of larger scatterers). In these experiments, for the sake of convenience, measurements were taken at a single angle; but instrumental effects have been carefully excluded (Pusey *et al.*, 1974), and it is felt that the special nature of the sample preparation precludes the possibility of sample-specific effects. The cumulants method of data analysis (Koppel, 1972) was used to confirm the single exponential behavior predicted by eq 5.

The operation of the correlator is similar to that of Foord *et al.* (1970), and has been described previously (Koppel, 1973; Pusey *et al.*, 1974).

Results

Direct Results: Intensity Profiles, Sedimentation Coefficients, Diffusion Coefficients. Figure 2 presents the results of experiments on a ribosome sample in buffer I. Experimental values of the total scattered intensity (expressed here as photocounts per second) are displayed as a function of r, the distance from the axis of rotation in the centrifuge during centrifugation. The sedimentation coefficients at the top were calculated for a particle density (Hill *et al.*, 1969a) $\rho_p = (\bar{v})^{-1} = 0.60^{-1}\ \text{g cm}^{-3} = 1.67\ \text{g cm}^{-3}$, interpolating between the values for 1.60 and 1.70 g cm^{-3} (McEwen, 1967). The principal peak is thus seen to correspond to the 70S ribosomes, with a secondary peak of 50S subunits. The diffusion coefficients measured by photocount autocorrelation and normalized to standard conditions (water as solvent at 20°) are presented for each peak. All diffusion measurements were performed at 5°, with a scattering angle of 90°, and an incident wavelength of 5682 Å.

As an example of raw correlator data, the normalized counter contents, C_m/N, for the correlation data of the 70S peak is presented in Figure 3a. Here

$$C_m = \sum_{i=1}^{N} n_0^{(8)}(t_i)n(t_i + mT) \tag{6}$$

with $\langle n\rangle = 0.723$, $T = 40\ \mu\text{sec}$, and $N = 2.444 \times 10^7$. The dashed line is the measured normalized background correlation level

$$B/N \equiv N^{-2} \sum_{i=1}^{N} n_q^{(s)}(t_i) \sum_{j=1}^{N} n(t_j) \tag{7}$$

Figure 3b shows the natural logarithm of the signal above background

$$k(mT) = {}^1/_2 \ln (C_m - B) \tag{8}$$

The ordinate

$$\tau^* = [(T_0 + T)/(T_0 + 20°)](\eta_{20,\text{w}}/\eta_{T,\text{s}})K^2\tau \tag{9}$$

where $T_0 = 273.15$°K, is defined so that the slope of the straight-line fit (solid line) is the measured value of $D_{20,\text{w}}$.

---

[4] The field scattered by a large number of independent scatterers obeys Gaussian statistics (Schaefer and Pusey, 1972).

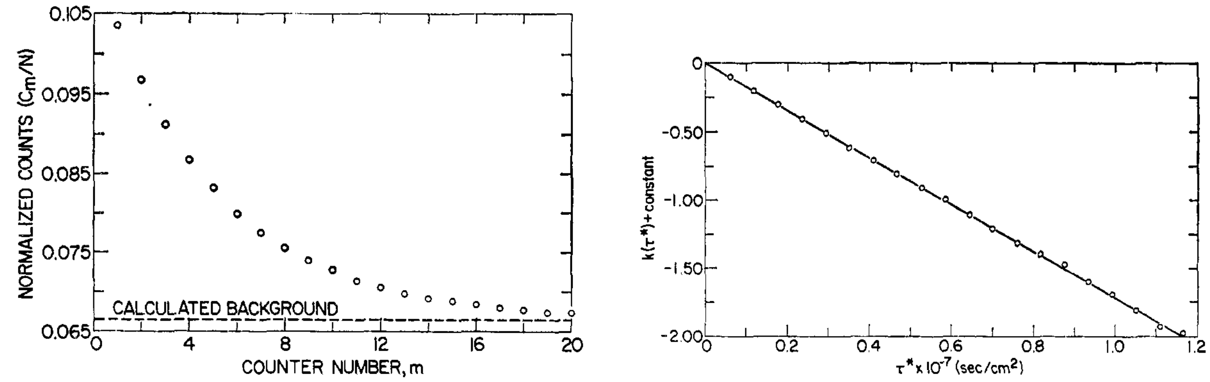

FIGURE 3: (a, left) Normalized counter contents of 70S correlation data of the sample of Figure 2. Horizontal dashed line is the normalized background correlation level, calculated from measured values of $\langle n_q^{(s)} \rangle$ and $\langle n \rangle$. (b, right) Natural logarithm of the signal above background. Solid line is the best least-squares straight-line fit.

In Figure 4 we have the results of three samples of ribosome subunits in buffer II. The 70S ribosomes are seen to be completely dissociated. These samples were prepared from the same ribosome stock solution, with 4b and 4c run with twofold and fourfold dilutions of the solution used in 4a. The peaks in 4a are quite broad and asymmetric; but inasmuch as this effect is seen to decrease in 4b and 4c, it is more likely attributable to concentration-dependent sedimentation characteristics than sample polydispersity. This is borne out by the diffusion measurements.

In addition to peaks at 50 and 30 S, there is a distinct third peak at about 25 S. This peak evidently is composed of the 25S partially unfolded form of the 30S subunit observed by others (Gesteland, 1966). In support of this, we observe that the ratios S/D are approximately the same for the 30S and 25S peaks, indicating a change of conformation without loss of mass. This would also explain why the 30S peak is somewhat smaller, relative to the 50S peak, than would otherwise be expected.

Diffusion coefficients were measured at several positions in each gradient. In this way one can check the homogeneity of a peak, or alternately, measure D as a function of concentration in one sample.

Figure 5 presents a compilation of diffusion measurements as a function of ribosome concentration. Concentrations were determined by the method outlined above. (See the Appendix, however.) Values of cM are determined from relative scattered intensities, and corrected to c using the values of M calculated below. Two points in Figure 5 deserve special attention. The 50S point with the Δ was measured in buffer I (the high Mg buffer). It is somewhat higher than the others, but agrees within experimental error. The 70S point with the open square was measured outside a gradient in regular buffer. This value of D confirms the accuracy of the gradient calibration, and assures us that the high concentration of sucrose has not induced a conformational change. At ribosome concentrations as low as these (<1 mg/ml) the values of $D_{20,\mathrm{w}}$, in agreement with theoretical expectations (Pusey *et al.*, 1972; Altenberger and Deutch, 1973), show no detectable concentration dependence. Thus, the averages of the values in Figure 5 (the horizontal lines) are taken as the zero concentration values, $D_{20,\mathrm{w}}{}^0$, and are listed in Table I, along with the corresponding hydrodynamic radii.[5] These are (1.71 ± 0.03) × 10^{-7} cm²/sec and 126 ± 2 Å for the 70S ribosome; (1.90 ± 0.03) × 10^{-7} cm²/sec and 113 ± 2 Å for the 50S subunit; and (2.18 ± 0.03) × 10^{-7} cm²/sec and 98 ± 2 Å for the 30S subunit.

Derived Results: Molecular Weights, Shape, and Hydration. The molecular weights were calculated using the relationship of Svedberg (Svedberg and Pederson, 1940)

$$M = RTs_{20,\mathrm{w}}{}^0/D_{20,\mathrm{w}}{}^0(1 - \rho\bar{v}) \tag{10}$$

where R is the gas constant, T is 293°K, and ρ is the density of water at 20°. The values used for $s_{20,\mathrm{w}}{}^0$ and $\bar{v}$ are listed in Table I. All of these were taken directly from the literature. The resulting values of M, (2.49 ± 0.06) × 10^6 for the 70S ribosome,

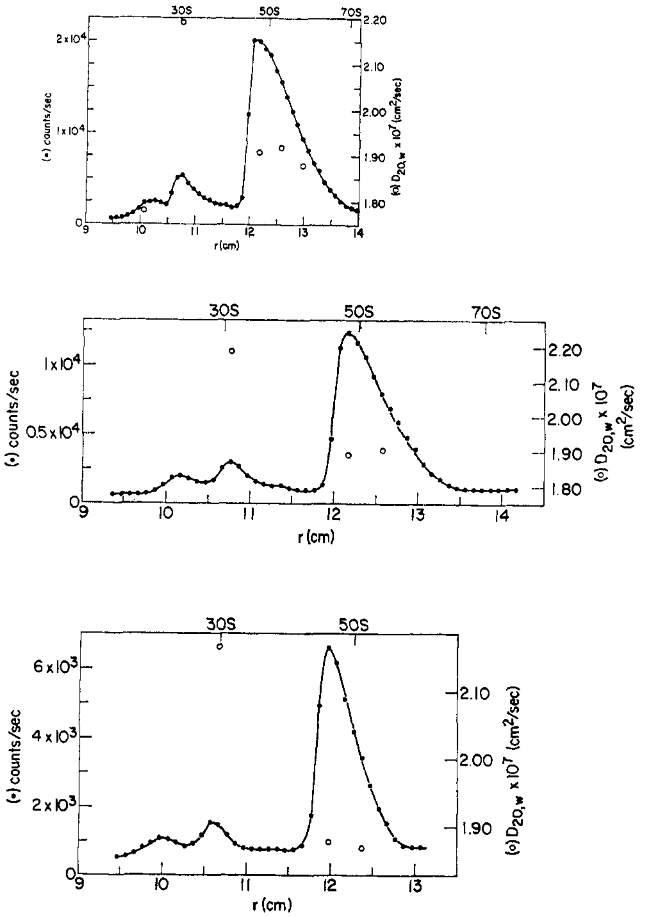

FIGURE 4: Three samples in sucrose gradients in buffer II, with initial ribosome concentrations in the ratio of 4:2:1.

---

[5] R_h is determined *via* the Stokes-Einstein equation, $R_\mathrm{h} = k(T_0 + T)/6\pi\eta_{T,\mathrm{s}}D_{T,\mathrm{s}}$ (k is the Boltzman's constant), and is the radius of the hydrodynamically equivalent sphere (equivalent as far as translational diffusion is concerned).

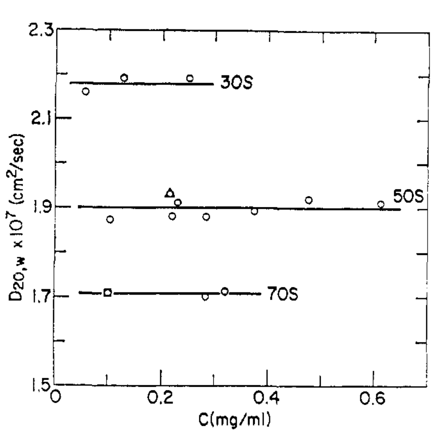

FIGURE 5: Measured values of $D_{20,w}$ as a function of ribosome concentration: (△) measured in sucrose gradient in buffer I; (□) measured in sucrose free buffer I preparation.

$(1.55 \pm 0.04) \times 10^6$ for the 50S subunit, and $(0.87 \pm 0.02) \times 10^6$ for the 30S subunit, are listed in Table I.

For any macromolecule, we can define the dry radius, R_d, as

$$R_d = (3M\bar{v}'/4\pi N)^{1/3} \qquad (11)$$

where $\bar{v}'$ is the inverse of the dry density of the macromolecule and N is Avogadro's number. The ratio of the hydrodynamic radius, R_h, to the dry radius, R_d, is a function of both the solvation and the degree by which the shape deviates from a sphere. We have (Camerini-Otero *et al.*, 1974)

$$R_h/R_d = (f/f_0)(1 - F)^{-1/3} \qquad (12)$$

where $(f/f_0) \geq 1$ represents the effect of shape on the frictional coefficient, and $(1 - F)^{-1}$ is the ratio of the solvated to dry volume. F, then, is the fraction of the volume of the hydrated molecule occupied by solvent. Explicit expressions for f/f_0 have been calculated for an ellipsoid of revolution as a function of axial ratio (Tanford, 1961). Figure 6 shows the combinations of axial ratio and F of the hydrodynamically equivalent ellipsoids of revolution, consistent with our measurements, for the 70S, 50S, and 30S ribosomes. (Oblate ellipsoids are presented with an axial ratio of less than 1, prolate ellipsoids with an axial ratio greater than 1.) Values of R_d were calculated from eq 11 using the values of M calculated above, and the values of $\bar{v}$ of Table I for $\bar{v}'$. We can alternatively characterize the degree of solvation with the parameter δ, the

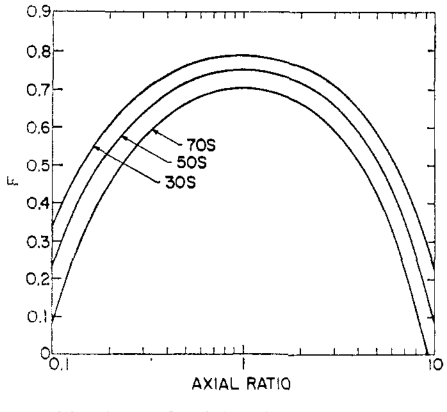

FIGURE 6: Combinations of axial ratio and F, the fraction of the total particle volume occupied by solvent, consistent with the calculated values of R_h/R_d.

TABLE I: Summary of Results.

	$D_{20,w}^0 \times 10^7$ (cm^2/sec)	R_h (Å)	$s_{20,w}^0 \times 10^{13}$ [a] (sec)	$\bar{v}$ (cm^3/g)[b]	$M \times 10^{-6}$	R_h/R_d	F_{max}	δ_{max} (cm^3/g)	F[c]	δ[c] (cm^3/g)
70 S	1.71 ± 0.03	126 ± 2	70.5 ± 0.7	0.596 ± 0.006	2.49 ± 0.06	1.50 ± 0.02	0.70 ± 0.01	1.41 ± 0.02	0.63	1.01
50 S	1.90 ± 0.03	113 ± 2	50.2 ± 0.5	0.585 ± 0.006	1.55 ± 0.04	1.59 ± 0.02	0.75 ± 0.01	1.75 ± 0.03	0.72	1.49
30 S	2.18 ± 0.03	98 ± 2	31.8 ± 0.3	0.591 ± 0.006	0.87 ± 0.02	1.67 ± 0.02	0.79 ± 0.01	2.18 ± 0.03	0.66	1.15

[a] Hill *et al.* (1969b). [b] Hill *et al.* (1969a). [c] See text.

volume of solvent per unit weight of dry macromolecule. Clearly

$$\delta = \bar{v}'[F/(1 - F)] \quad (13)$$

In Table I we present calculated values of R_h/R_d, F_{max}, and δ_{max}, where F_{max} and δ_{max} are calculated with an assumed spherical shape ($(f/f_0) = 1$).

We can further quantitate this hydration *via* eq 12 or Figure 6, by taking the particle shapes in solution as determined by low-angle X-ray diffraction (see Table II). This procedure gives values of F of 0.63, 0.72, and 0.66, and values of δ (in cm^3/g) of 1.01, 1.49, and 1.15 for the 70S ribosome and the 50S and 30S subunits, respectively, summarized in Table I.

Discussion

Diffusion Coefficients. In their pioneering physiochemical study of *E. coli* ribosomes, Tissierès *et al.* measured the diffusion coefficients by the classical method, observing free diffusion at a preformed concentration boundary (Tissierès *et al.*, 1959). Molecules must diffuse over macroscopic distances in this technique, and each measurement subsequently takes 2 or 3 days. They made a total of seven such measurements, obtaining values for $D_{20,w} \times 10^7$ of 1.82 and 1.84 cm^2 per sec for the 70S ribosomes; 1.88, 1.90, and 1.95 cm^2 per sec for the 50S subunit; and 2.81 and 3.10 cm^2 per sec for the 30S subunit.

For the 50S subunit, we find, perhaps coincidentally, a remarkable agreement between their values of D and those reported here. For the 70S ribosome, and especially for the 30S subunit, however, their values are significantly higher. This difference is in the direction that one would expect, since in the boundary diffusion method all thermal and vibrational disturbances in the course of the 2- to 3-day run time lead to a larger apparent D.

The diffusion coefficient of the 50S subunit has also been measured in a boundary diffusion experiment by Serdyuk *et al.* (1970). Their value of $(1.87 \pm 0.04) \times 10^{-7}$ cm^2/sec is in excellent agreement with the value reported here.

Hocker *et al.* (1973) have performed a series of IFS experiments on ribosome solutions with different added concentrations of KCl. Their principal objective was the observation of changes (on the time scale of days) in the state of aggregation of highly polydisperse solutions. Thus their determinations of individual diffusion coefficients were always complicated by the presence of a considerable fraction of aggregated material. Nevertheless, their reported values of $D_{20,w}$ ($1.53 \pm 0.1 \times 10^{-7}$ cm^2/sec for the 70S ribosome, and $1.84 \pm 0.1 \times 10^{-7}$ cm^2/sec for the 50S subunit) are in substantial agreement with those of this study.

Molecular Weights. The molecular weights calculated here have an internal consistency. The calculated sum of the molecular weights of the subunits, $(2.42 \pm 0.05) \times 10^6$, agrees with the calculated 70S molecular weight, $(2.49 \pm 0.06) \times 10^6$. We also find, however, a complete agreement between these molecular weights and those obtained by Hill *et al.* (1969a) with the method of sedimentation equilibrium: $(2.65 \pm 0.2) \times 10^6$, $(1.55 \pm 0.05) \times 10^6$, and $(0.90 \pm 0.03) \times 10^6$ for the 70S, 50S, and 30S ribosomes, respectively, calculated, incidently, with the same values of $\bar{v}$ used here. $\bar{v}$, moreover, enters into the two methods of determining M (sedimentation equilibrium and sedimentation diffusion), in the identical fashion, as a factor of $(1 - \rho\bar{v})^{-1}$. From their values for the molecular weights, Hill *et al.* speculated that the 70S ribosome might contain $\sim 2 \times 10^5$ daltons of material in excess of the simple sum of the 30S and 50S subunits. The molecular weights calculated here, however, make a difference of this magnitude highly unlikely.

Our molecular weights are somewhat smaller than those obtained by conventional light intensity measurements (Scafati *et al.*, 1971); $(2.9 \pm 0.3) \times 10^6$, $(1.7 \pm 0.1) \times 10^6$, and $(1.0 \pm 0.1) \times 10^6$, for the 70S, 50S, and 30S ribosomes, respectively. The results of that study, however, must be viewed with a certain amount of suspicion. The magnitude of the angular dependence of the scattered intensity exhibited there, in sample Zimm plots, is characteristic of scatterers an order of magnitude too large.

Size, Shape, and Hydration. It is of some interest to compare the values of R_h measured here, a parameter which combines the effects of both molecular size and shape, with the results of other physical techniques. Electron microscopy (Hall and Slater, 1959; Huxley and Zubay, 1960; Hart, 1962; Spirin *et al.*, 1963) and low-angle X-ray (Hill *et al.*, 1969b) studies have yielded values for the ribosome molecular dimensions. These are summarized in Table II, along with calculated values of R^{eq}, R^{eq}/R_d, R_h^{eq}, and R_h/R_h^{eq}. R^{eq} is the radius of the sphere of equal volume. Volumes were calculated for assumed ellipsoidal shapes, except for the X-ray dimensions of the 70S ribosomes where the scattering data were fit to an ellipsoidal cylinder. R_d is the dry radius calculated above (see Table I). R_h^{eq} is the equivalent hydrodynamic radius, the value of R_h that a particle of these dimensions would have. Thus

$$R_h^{eq} = (f/f_0)R^{eq} \quad (14)$$

where (f/f_0), again, represents the effect of shape on the frictional coefficient.

It is clear from the values of R^{eq}/R_d and R_h/R_h^{eq} in Table II that the dimensions obtained by electron microscopy, with the single exception of the 50S measurements of Hart (1962), are much closer to those of the theoretical compacted dry particle than they are to the hydrodynamic dimensions in solution. This, perhaps, is to be expected. Hart studied freeze-dried ribosome samples, but all of the other experimenters used air-dried preparations.

TABLE II: Ribosome Dimensions.

	Dimensions (Å)	R^{eq} (Å)	R^{eq}/R_d	R_h^{eq} (Å)	R_h/R_h^{eq}
70 S	$170 \times 200 \times 200^a$	95	1.13	96	1.31
	$160 \times 180 \times 200^b$	90	1.07	91	1.39
	$150 \times 150 \times 190^d$	81	0.97	82	1.30
	$135 \times 200 \times 400^e$	127	1.51	137	0.92
50 S	$140 \times 170 \times 170^a$	80	1.13	81	1.39
	$150 \times 150 \times 150^b$	75	1.06	75	1.51
	$160 \times 230 \times 230^c$	102	1.44	100	1.13
	$150 \times 150 \times 150^d$	75	1.06	75	1.51
	$130 \times 170 \times 310^e$	95	1.34	100	1.31
	$115 \times 230 \times 230^e$	91	1.28	95	1.19
30 S	$95 \times 95 \times 170^a$	58	0.99	60	1.63
	$70 \times 180 \times 180^b$	66	1.13	71	1.38
	$80 \times 120 \times 140^d$	55	0.94	56	1.75
	$55 \times 220 \times 220^e$	70	1.19	82	1.19

[a] Hall and Slater (1959). [b] Huxley and Zubay (1960). [c] Hart (1962). [d] Spirin *et al.* (1963). [e] Hill *et al.* (1969b).

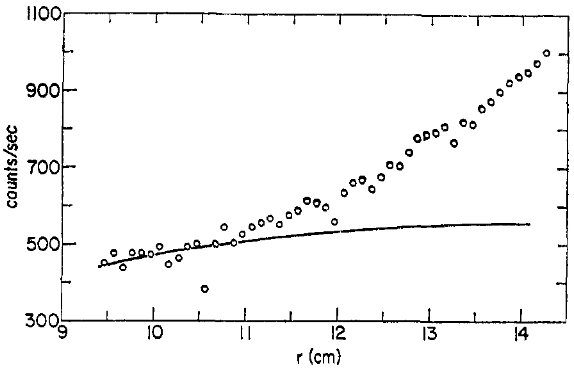

FIGURE 7: Intensity scan of a centrifuged ($\int\omega^2 dt = 2.343 \times 10^{11}$ sec^{-1}) blank sucrose gradient. Solid line is the intensity for sucrose alone, calculated from osmotic pressure data, scaled to fit the measured intensities near the top of the tube.

The large values of R_h/R_h^{eq} for the air-dried samples offers additional evidence, independent of determinations of M and $\bar{v}$, of the extensive hydration of the ribosomes in solution. The magnitude of this "hydrodynamic hydration" differs considerably from the relatively low values (0.33 g/g for the 70S ribosomes, 0.39 g/g for a mixture of subunits) obtained using a technique of low-temperature nuclear magnetic resonance (White *et al.*, 1972). Most of the hydrodynamic hydration, evidently, consists of entrapped bulk solvent, and thus is not detected by the criteria of the nuclear magnetic resonance technique. The magnitude of this hydration is consistent, however, with that found by Tolbert (1971) and Smith (1971), (1.3–1.4 g/g for the 30 S, and 1.38 g/g for the 50 S, respectively), and comparable to those found in similar IFS experiments on a series of different spherical viruses (Camerini-Otero *et al.*, 1974).

R_h is also significantly larger than the low-angle X-ray R_h^{eq} for the 50S and 30S subunits in solution. (The 70S dimensions agree quite well; but this agreement is probably coincidental. Hill *et al.* (1969b) observed evidence of extensive dimerization of the 70S ribosomes, which led them to believe that their 70S dimensions overestimated the size of the particle.) While it is true that the X-ray measurements would not include external layers of hydration which would affect the hydrodynamic measurements, these layers would have to extend as far as 13–18 Å from the particle surface to reconcile the differences between R_h and R_h^{eq}. This might indeed be the case (Tolbert, 1971; Smith, 1971), but recent IFS studies of virus solutions speak against such an external hydration beyond one or two layers of water molecules (Camerini-Otero *et al.*, 1974). Perhaps the effect arises from deviations from the assumed uniform particle electron density (Serdyuk *et al.*, 1970). This could be the result of a nonuniform distribution of protein and RNA within the nucleoprotein particle. Neutron scattering studies of the 50S subunit, in fact, have found a 58 Å separation between the centers of mass of the protein and RNA moieties (Moore *et al.*, 1974). Invaginations of the ribosome surface, such as those observed in the structure of certain viruses (Crowther and Amos, 1972), would also decrease the density near the surface resulting in smaller low-angle X-ray effective particle dimensions, without affecting the hydrodynamic properties of the particles (Camerini-Otero *et al.*, 1974).

Concluding Remarks

Used together in tandem in a single experiment, band velocity centrifugation and intensity fluctuation spectroscopy form a new, effective, general analytical technique. In a single experiment, one can determine the sedimentation coefficient, diffusion coefficient, molecular weight, and concentration of each of the macromolecular solute components. If values of the particle density are not known and cannot be estimated from the chemical composition, they can be obtained in two runs with sucrose gradients with different values of the parameter $Z_0 = Z(r = 0)$. If two peaks cannot be completely resolved, or if there is a broad continuous distribution of molecular size, analysis can proceed with measurements of the z-average D, and perhaps higher order moments of D as well, as a function of position (Koppel, 1972). Thus, while this combination of techniques can be used with highly purified, well-characterized systems, with the band centrifugation acting primarily as a preparative technique for the subsequent light-scattering experiment, its greatest potential lies, perhaps, in the initial characterization of complicated multicomponent systems.

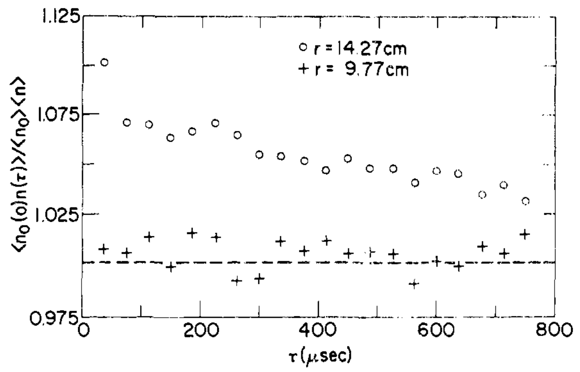

FIGURE 8: Correlation data, normalized by the calculated background, measured at two points in the sucrose gradient of Figure 7.

Acknowledgments

Thanks are due in large measure to the faculty and staff of both the Columbia University Physics Department and the IBM Thomas J. Watson Research Center for making this work possible. First and foremost, I wish to thank Dr. Seymour H. Koenig for the guidance, support, and freedom necessary for a successful graduate education. Special thanks are due to Drs. Peter N. Pusey and Dale W. Schaefer for sharing their insights, experience, and friendship. I am also pleased to acknowledge the key assistance of Dr. Charles Cantor and Ms. Helen Oen of the Columbia University Department of Chemistry. Finally, I wish to express my sincere appreciation to all the people of the IBM Watson Laboratory and the General Sciences Department of the IBM Thomas J. Watson Research Center for making my work there a both rewarding and enjoyable experience.

Appendix: Sucrose Contaminants

As detailed above, values of cM can be determined from relative scattered intensities with the aid of a sucrose light-scattering standard. An additional effect, however, has to be taken into account. Figure 7 shows an intensity scan of a "blank" sucrose gradient centrifuged at 25 krpm for 9 hr. The solid line is the expected counting rate due to light scattered by the sucrose, obtained from osmotic pressure data, and scaled to fit the data here near the top of the tube. There is, evidently, a small amount of a large contaminant of some sort that has mostly centrifuged to the bottom of the tube. This is borne out by the correlation data of Figure 8. At $r = 14.27$

cm, the measured correlation function is significantly above background for delay times of the order of 10^{-8} sec. No such correlations are seen at $r = 9.77$ cm. Correlations, moreover, are found at all positions in an uncentrifuged gradient (but not in buffer alone) and can be shown to scale as K^2T/η. The relative intensities are such, however, that the presence of this component in the centrifuged sample did not significantly affect the measured values of D.

Similar contaminants have been reported by Greenberg *et al.* (1973), and analyzed as polysaccharides, possibly amylose or cellulose (Turner and Zust, 1973).

References

Altenberger, A. R., and Deutch, J. M. (1973), *J. Chem. Phys. 59*, 894.

Camerini-Otero, R. D., Pusey, P. N., Koppel, D. E., Schaefer, D. W., and Franklin, R. M. (1974), *Biochemistry 13*, 960.

Chu, B. (1970), *Annu. Rev. Phys. Chem. 21*, 145.

Clark, N. A., Lunacek, J. H., and Benedek, G. B. (1970), *Amer. J. Phys. 38*, 575.

Crowther, R. A., and Amos, L. A. (1972), *Cold Spring Harbor Symp. Quant. Biol. 36*, 489.

Cummins, H. Z., Carlson, F. D., Herbert, T. J., and Woods, G. (1969), *Biophys. J. 9*, 518.

Cummins, H. Z., and Swinney, H. L. (1970), *Progr. Opt. 8*, 133.

Debye, P. (1947), *J. Phys. Colloid. Chem. 51*, 18.

Foord, R., Jakeman, E., Oliver, C. J., Pike, E. R., Blagrove, R. J., and Peacocke, E. (1970), *Nature (London) 227*, 242.

Fujime, S. (1970), *J. Phys. Soc. Jap. 29*, 751.

Gesteland, R. F. (1966), *J. Mol. Biol. 18*, 356.

Ghysen, A., Bollen, A., and Herzog, A. (1970), *Eur. J. Biochem. 13*, 132.

Greenberg, J. R., Kelley, D. E., Perry, R. P., and Rartof, K. D. (1973), *Science 181*, 186.

Hall, C. E., and Slater, H. S. (1959), *J. Mol. Biol. 1*, 329.

Handbook of Biochemistry (1972), Sober, H. A., Ed., Cleveland, Ohio, The Chemical Rubber Co., 2nd ed, p J-288.

Handbook of Chemistry and Physics (1972), Weast, R. C., Ed., Cleveland, Ohio, The Chemical Rubber Co., 53rd ed, p E-211.

Hart, R. G. (1962), *Biochim. Biophys. Acta 60*, 629.

Hill, W. E., Anderegg, J. W., and Van Holde, K. E. (1970), *J. Mol. Biol. 53*, 107.

Hill, W. E., Rosetti, G. P., and Van Holde, K. E. (1969a), *J. Mol. Biol. 44*, 263.

Hill, W. E., Thompson, J. D., and Anderegg, J. W. (1969b), *J. Mol. Biol. 44*, 89.

Hocker, L., Krupp, J., Benedek, G. B., and Vournakis, J. (1973), *Biopolymers 12*, 1677.

Huxley, H. E., and Zubay, G. (1970), *J. Mol. Biol. 2*, 10.

International Critical Tables (1928), Wasburn, E. W., Ed., New York, N. Y., McGraw-Hill, Vol. IV, p 429.

Jakeman, E., Oliver, C. J., Pike, E. R., and Pusey, P. N. (1972), *Proc. Phys. Soc. London (Gen.) 5*, L93.

Jakeman, E., and Pike, E. R. (1969), *Proc. Phys. Soc. London (Gen.) 2*, 411.

Koppel, D. E. (1971), *J. Appl. Phys. 42*, 3216.

Koppel, D. E. (1972), *J. Chem. Phys. 57*, 4814.

Koppel, D. E. (1973), Ph.D. Thesis, Columbia University.

Koppel, D. E., and Schaefer, D. W. (1973), *Appl. Phys. Lett. 22*, 36.

Kurland, C. G. (1972), *Annu. Rev. Biochem. 41*, 377.

McEwen, C. R. (1967), *Anal. Biochem. 20*, 114.

Moore, P. B., Engleman, D. M., and Schoenborn, B. P. (1974), *Proc. Nat. Acad. Sci. U. S. 71*, 172.

Pecora, R. (1964), *J. Chem. Phys. 40*, 1604.

Pecora, R. (1965), *J. Chem. Phys. 43*, 1562.

Pecora, R. (1968), *J. Chem. Phys. 48*, 4126.

Pusey, P. N., Koppel, D. E., Schaefer, D. W., Camerini-Otero, R. D., and Koenig, S. H. (1974), *Biochemistry 13*, 952.

Pusey, P. N., Schaefer, D. W., Koppel, D. E., Camerini-Otero, R. D., and Franklin, R. M. (1972), *J. Phys. Radium 33*, C1–163.

Scafati, A. R., Stornaiuolo, M. R., and Novaro, P. (1971), *Biophys. J. 11*, 370.

Schaefer, D. W., Benedek, G. B., Schofield, P., and Bradford, E. (1971), *J. Chem. Phys. 55*, 3884.

Schaefer, D. W., and Pusey, P. N. (1972), *Phys. Rev. Lett. 29*, 843.

Serdyuk, I. N., Smirnov, N. I., Ptitsyn, O. B., and Fedorov, B. A. (1970), *FEBS (Fed. Eur. Biol. Soc.) Lett. 9*, 324.

Smith, W. S. (1971), Ph.D. Thesis, University of Wisconsin.

Spirin, A. S. (1969), *Progr. Biophys. Mol. Biol. 19*, 133.

Spirin, A. S., and Gavrilova, L. P. (1969), The Ribosome, New York, N. Y., Springer Verlag.

Spirin, A. S., Kiselev, N. A., Shakulov, R. S., and Bogdanov, A. A. (1963), *Biokhimiya 28*, 920.

Svedberg, T., and Pederson, K. O. (1940), The Ultracentrifuge, New York, N. Y., Oxford University Press.

Tanford, C. (1961), Physical Chemistry of Macromolecules, New York, N. Y., Wiley, Chapter 6.

Tissierès, A., Watson, J. D., Schlessinger, D., and Hollingworth, B. R. (1959), *J. Mol. Biol. 1*, 221.

Tolbert, W. R. (1971), Ph.D. Thesis, University of Wisconsin.

Traub, P., Mizushima, S., Lowry, C. B., and Nomura, M. (1971), *Methods Enzymol. 20*, 391.

Turner, S. C., and Zust, J. R. (1973), *Science 181*, 186.

White, J. P., Kuntz, I. D., and Cantor, C. R. (1972), *J. Mol. Biol. 64*, 511.

Zamir, A., Miskin, R., and Elson, D. (1971), *J. Mol. Biol. 60*, 347.